Estimation of Wildfire Size and Location Using a Monocular Camera on a Semi-autonomous Quadcopter

de Paula, Lucas Goncalves; Hyttel, Kristian; Geipel, Kenneth Richard; de Domingo Gil, Jacobo Eduardo; Novac, Iuliu; Chrysostomou, Dimitrios

Published in:
Computer Vision Systems

DOI (link to publication from Publisher):
10.1007/978-3-030-34995-0_13

Publication date:
2019

Document Version
Accepted author manuscript, peer reviewed version

Citation for published version (APA):
de Paula, L. G., Hyttel, K., Geipel, K. R., de Domingo Gil, J. E., Novac, I., & Chrysostomou, D. (2019). Estimation of Wildfire Size and Location Using a Monocular Camera on a Semi-autonomous Quadcopter. In D. Tzovaras, D. Giakoumis, M. Vincze, & A. Argyros (Eds.), Computer Vision Systems : 12th International Conference, ICVS 2019, Thessaloniki, Greece, September 23–25, 2019, Proceedings (pp. 133-142). Springer. https://doi.org/10.1007/978-3-030-34995-0_13

Estimation of Wildfire Size and Location using a Monocular Camera on a Semi-Autonomous Quadcopter

Lucas Goncalves de Paula[1], Kristian Hyttel[1], Kenneth Richard Geipel[1], Jacobo Eduardo de Domingo Gil[1], Iuliu Novac[1], and Dimitrios Chrysostomou[2][0000−0002−6114−8944]

[1] Department of Materials and Production, Aalborg University
Fibigerstraede 16, Aalborg East, DK-9220, Denmark
[2] Robotics and Automation Group, Department of Materials and Production
Aalborg University, Fibigerstraede 16, Aalborg East, DK-9220, Denmark
http://robotics-automation.aau.dk/

Abstract. This paper addresses the problem of estimating the location and size of a wildfire, within the frame of a semi-autonomous recon and data analytics quadcopter. We approach this problem by developing three different algorithms, in order to accommodate this problem. Two of these taking into the account that the middle of the camera's FOV is horizontal with respect to the drone it is mounted. The third algorithm relates to the bottom point of the FOV, directly under the drone in 3D space. The evaluation shows that having the pixels correlate to ratios in percentages rather than predetermined values, with respect to the edges of the fire, will result in better performance and higher accuracy. Placing the monocular camera horizontally in relation to the drone will provide an accuracy of 68.20%, while mounting the camera with an angle, will deliver an accuracy of 60.76%.

Keywords: Wildfire Recognition · Quadcopter Analytics · Image Processing · Area Estimation.

1 Introduction

As the frequency of extreme weather increases and become more violent due to climate change [6], so does the initial attack success of wildfires [9]. Emergency response personnel, across the globe, struggle to contain the increase of wildfire size, numbers and severity. In the summer of 2018, California experienced the largest wildfire in the state's history [8], in Sweden emergency personnel were overwhelmed by the numbers of forest fires [12], and in Greece, two violent fires left 250 injured and 105 dead [4]. Considering this, emergency services are investigating how flying robotic technologies can facilitate a faster and more accurate data gathering procedure from wildfires, to increase the efficacy of firefighting operations [11, 3].

The needs of firefighters combatting wildfires were determined through a collaboration with the Danish Emergency Management Agency, DEMA and interviews with Evan Bek Jensen, the second in command of the Herning drone unit. Discussing a potential new product versus current methods, it became evident that the location, size, intensity and direction of a wildfire were essential for better allocation of their resources. This can be achieved by developing a semi-autonomous quadcopter, that will be controlled remotely via a handheld device. An area of interest is provided as input to the quadcopter by the operator, which later autonomously explores the area. The proposed solution utilizes MobileNet v2 [10], a deep convolutional neural network architecture, as well as a custom built database for recognition and processing of the data of the wildfire, in regards to previous mentioned needs. The contribution of this work lies on the use of a monocular camera for fast calculation and accurate estimation of the location and size of the wildfire area, by comparing the nearest and farthest detected point of the fire with respect to the quadcopter's GPS location.

1.1 Related Works

A number of systems have been developed in order to triangulate the location of a wildfire, most of these include multiple sensors in order to get an accurate location of the fire. One study group recorded the same fire or smoke from different angles. Comparing the position of the sources recording the fire and key terrain features to each other using four sensors, two UAVs and two ground based cameras [2]. Another work used multiple sensors, mounted on three UAVs, and compared the location according to each of the UAVs while recorded the contour of the fire, in order to predict the direction of the fire spread [7]. Recently, Amanatiadis et al. introduced a realtime surveillance detection system for UAVs based on GPGPUs and FPGAs enabling the accurate and fast detection of ambiguous objects [1]. As the presented work is based on a low-cost, commercial drone, the on board computation is kept at minimum due to lack of computational resources and weight restrictions on the drone.

Further Studies in regards to fire recognition have been achieved via a consumer grade monocular camera system. Merino et al. were able to detect wildfire, but also predict its development with regards to vegetation or burned area [5]. Furthermore, Yuan et al. showed that detecting fire can be based not only on the fire palette, but also on the optical flow of the moving flames [13]. Additionally, Zhao et al. presented a novel 15-layered self-learning deep learning architecture to extract fire features and successfully classify them as wildfire [14]. The work presented in this paper will combine elements of these different approaches by detecting the fire using a deep convolutional neural network and later estimate the size and location using a monocular low-budget camera mounted on a quadcopter.

1.2 System Description

The system used for this work relies on an open-source quadcopter, the Intel Aero Ready-To-Fly drone coupled with the Intel Realsense R-200 RGBD camera (Fig. 1). In order to have the computational power needed to process the acquired data, a computer will act as a master, although the system is controlled by an intuitive user interface on the handheld device. Figure 2 illustrates the system's functionalities. Upon arriving at the site of an emergency, the quadcopter's operator in collaboration with the incident commander, identifies in which area the quadcopter must be put into action (Fig. 2a). Utilising the GUI on the tablet, the quadcopter's operator is presented with a topological map, to select an area of interest (Fig. 2b). The quadcopter autonomously flies to this area and begins an area search of a fire (Fig. 2c), flying in a snake pattern when arrives in the area of interest (Fig. 3a). In the incident of the detection of a wildfire, the quadcopter will stream the collected data to the master computer for further processing and calculation of the location, size, intensity and direction of the wildfire. This information will then be overlaid onto the topological map of the user interface, providing a current data interpretation for the firefighters to take into account when allocating resources (Fig. 2d).

2 Proposed method

Due to the collaboration with DEMA, video footage of real firefighting operations in Denmark, was obtained as Figure 3b depicts. This is footage from Dokkedal, Denmark, where a fire in a field is shown. DEMA operates with thermal imagery, and scans the area within a range of 80-800° Celsius, in order to eliminate any noise. In order to apply any calculation in regards to estimate the area of the fire, the algorithm will first determine the edges of the fire. The presented image, of a real wildfire, is required to be in grey scale, while the algorithm detects differences in intensity, and by utilising a dynamic threshold, it sets the edge pixel to 1 while non-edge to 0. Once the edges have been identified, the second part of the algorithm will calculate the distances to the edges, compared to that of the quadcopter's GPS position, in order to calculate the size of the fire.

(a) Intel Aero Ready-To-Fly Quadcopter

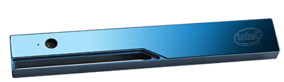

(b) Intel RealSense R200

(c) Microsoft Surface Go

Fig. 1: Hardware used for the setup of the project

(a) The firefighter arrives on site and assess the situation

(b) The firefighter selects the area of interest

(c) The quadcopter scans the selected area

(d) The operator receives a visual feedback of the fire's size and location

Fig. 2: Infographic of the stepwise process on the use of the developed framework

Figure 4 illustrates a general approach of this, visualized viewing from the side to highlight how this is calculated. The height of the quadcopter is represented with H which is known from the quadcopter's altitude sensor. Knowing two angles, and the altitude of the quadcopter, $L2 - L1$ represents the fire size and can be calculated by Equation 1.

$$L2 - L1 = tan(A2 + A1) * H - tan(A1) * H \tag{1}$$

Based on this, three algorithms were developed, gradually having more generic

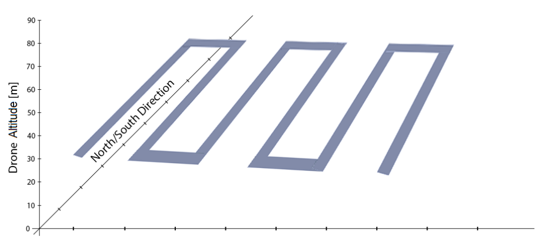

(a)

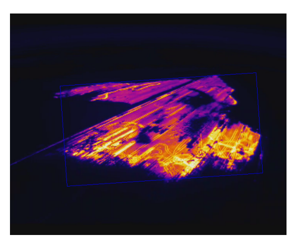

(b)

Fig. 3: (a) The quadcopter navigates in a snake pattern and (b) a snippet of thermal imagery provided by DEMA.

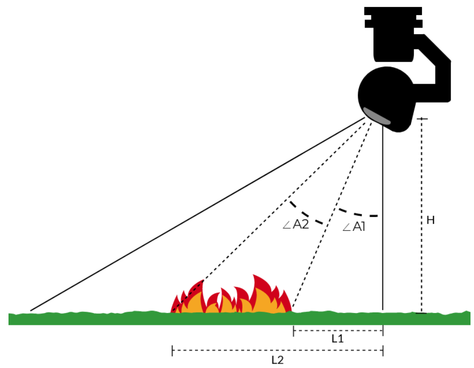

Fig. 4: Side View of the Fire Size Calculation

requirements, in order to calculate the location and the size of the detected wildfire, and determine the optimal way of extinguishing the wildfire. Figure 5 illustrates generic drone viewpoints for both front facing camera (Fig. 5a) and the angled camera (Fig. 5b) approaches with their correspondent total area seen by the drone.

Front-Facing Pixel Value Approach The first algorithm is based on the premise that the camera faces straightforward in front of the quadcopter, as originally mounted, which means that the upper half of the image does not capture the ground. As a result, only the bottom half of the image can be used, and the input image is cut in half, discarding the top half of the image. The lower half is then divided into 44 equally sized pieces. The lowest visible angle

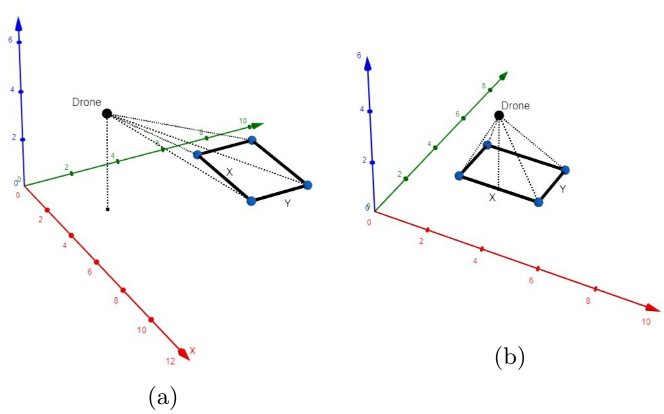

Fig. 5: Generic representation of proposed approaches and the respective coordinate frames

can be seen in Equation 2.

$$90^\circ - \frac{FOV}{2} = 68.5^\circ \tag{2}$$

The difference from 68.5° to 90° can be divided into 44 steps of 0.5°, hence why the lower half of the image is divided into 44 pieces. Each of these equal parts corresponds to a specific pixel value in the input image. The input images have a resolution of 1920×1080 pixels and since only half of each image is used, 540 pixels would be divided equally by 44. Each of these pieces will then be equally spaced by ≈ 12.53 pixels, see Table 1 for clarification. After finding the edges of the fire in the input image in the form of a pixel value, it will be correlated to the array of pixel values. After finding the pixel value in the table which has the smallest difference to the edge pixel values, the angle can be found in the row above. Using this angle, the distance to the fire can be found. The same approach is taken to find the end of the fire. These two distances are then subtracted to find the location and size of the fire.

Front-Facing Image Ratio Approach The second algorithm uses the same fundamental principles as the first, but it makes use of a different method to calculate the angle from the centre of the lens to the wildfire's edges. Instead of approximating the pixel value to an array of predetermined pixel values, the second algorithm makes use of the angle of the camera and ratios for increased accuracy. Equation 3 calculates a ratio of where the wildfire's initial position in relation to the height of the image, given as a percentage.

$$FireStart = 100 - \frac{\frac{FireEdgeStart}{ImageHeight}}{2} * 100 \tag{3}$$

Where, *FireEdgeStart* is the position of the pixel at which the fire starts and *ImageHeight* is the entire height of the input image. This value is subtracted

Angle	68.5°	69°	69.5°	70°	70.5°	71°	71.5°	72°	72.5°	73°
Pixel Value	1	12.53	25.06	37.6	50.13	62.67	75.2	87.74	100.27	112.81
Angle	73.5°	74°	74.5°	75°	75.5°	76°	76.5°	77°	77.5°	78°
Pixel Value	125.34	137.88	150.41	162.95	175.48	188.02	200.55	213.09	225.62	138.16
Angle	78.5°	79°	79.5°	80°	80.5°	81°	81.5°	82°	82.5°	83°
Pixel Value	250.69	263.23	275.76	288.3	300.83	313.37	325.9	338.44	350.97	363.51
Angle	83.5°	84°	84.5°	85°	85.5°	86°	86.5°	87°	87.5°	88°
Pixel Value	376.04	388.58	401.11	413.65	426.18	438.72	451.25	463.79	476.32	488.86
Angle	88.5°	89°	89.5°	90°						
Pixel Value	501.39	513.93	526.46	539						

Table 1: Angles and their Respective Pixel Values - The specific angle to each point is given by the first row in each line. The second row represents the pixel value of the above angle.

from 100 to find the ratio from the bottom of the image instead of the top. This is necessary because the origin of pixels in an image is in the top-left corner. This equation is calculated twice to find the initial and final position of the fire. Using these ratios, the angles related to the two points can be calculated with the Equation 4.

$$FireStartDeg = \frac{FireStart * \frac{FOV}{2}}{100} \tag{4}$$

Where, *FireStart* is the value of Equation 3 and FOV is the vertical field of view of the camera. This calculation is also done twice. The results are angles in degrees from the bottom of the image, which represents the point at which the fire starts and ends. After these two calculations have been completed, the distance to each point can be established using the trigonometric functions as shown in Equation 5.

$$FireDistStart = \tan(FireStartDeg + 68.5^{\circ}) * Height \tag{5}$$

Where, *FireStartDeg* is the result of Equation 4 and *Height* is the altitude of the quadcopter when the input image was taken. As it is necessary to take the part below the visible FOV of the camera into consideration, another 68.5° are added.

Angled Camera Image Ratio Approach The previously described algorithms have been based on the premise that the camera would point directly in front of the quadcopter, this algorithm is based on the camera's lowest FOV point aimed straight down from the quadcopter's position. Therefore, in the *Angle-Improved Image Ratio Approach*, the entire FOV of the camera can be used rather than only half. This is done due to the necessity to address the error that arises near the horizon of the input image. Consequently, the camera is now mounted onto the quadcopter using a 3D printed custom-made mount.

Consequently, the calculations used in *Front-Facing Pixel Value Approach* and *Front-Facing Image Ratio Approach* must be altered to accommodate for the increased FOV and change in angle. Equation 3 will then transform into Equation 6.

$$FireStart = 100 - \frac{FireEdgeStart}{ImageHeight} * 100 \tag{6}$$

Likewise, Equation 4 transform into the Equation 7.

$$FireStartDeg = FireStart * \frac{FOV}{100} \tag{7}$$

Equation 5 transforms in the following way, as the 68.5°, which was added, is now incorporated into the orientation of the camera and, therefore, should no longer be part of the equation, and will have the expression as seen in Equation 8.

$$FireDistStart = \tan(FireStartDeg) * Height \tag{8}$$

3 Evaluation

In order to evaluate the robustness and accuracy of the proposed algorithms, additional tests were required to correlate the data from the thermal imagery provided by DEMA, with the quadcopter's altitude, position and FOV data. A white blanket positioned in the middle of a field simulates an area of interest and acts as an input to the edge detection algorithm, Furthermore, the same test setup will be used for all three algorithms to compare the results and reflect the differences in accuracy. This test setup is shown in Figure 6a and 6b, as captured from the camera's perspective. As the camera is angled in algorithm 3, so the lowest point of the FOV correlates to the point directly under the quadcopter, the input image will therefore be as seen in Figure 6b from the camera's perspective.

(a) Test setup environments for the first two algorithms

(b) Test setup environment for the third algorithm

Fig. 6: Test setup environments for the proposed algorithms

3.1 Results

In order to evaluate the accuracy of the algorithms, the acquired results are shown in comparison to the estimated area and location of the test subject. The distribution of the calculated points of interest generated from the test of the *Front-Facing Pixel Value Approach*, are depicted in Figure 7a, and resulted in an accuracy of 46.06%. As the *Front-Facing Image Ratio Approach* does not attempt to match an angle to a pixel value, but rather uses a more precise ratio, the results were vastly improved. The resulting calculation provided an accuracy of 68.20%, and the respective distribution of the point of interest is illustrated in Figure 7b. Lastly, the distribution of the point of interest used for the *Angled Camera Image Ratio Approach* are highlighted in Figure 7c. Although this test differs from the first two, the resulting calculation of the area within the polygon corresponds to an accuracy of 60.76%.

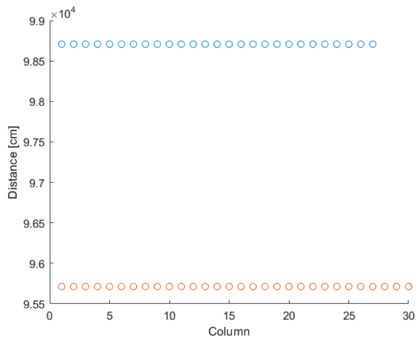

(a) Distribution of points of interest for the test of the *Front-Facing Pixel Value Approach*

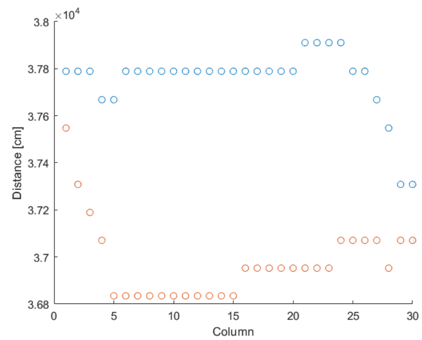

(b) Distribution of points of interest for the test of the *Front-Facing Image Ratio Approach*

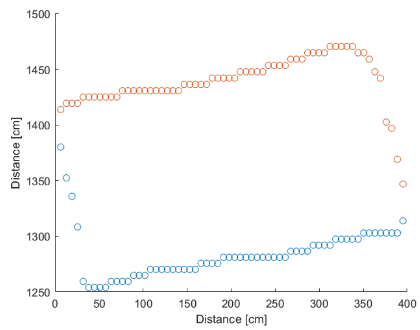

(c) Distribution of points of interest for the test of the *Angle-Improved Image Ratio Approach*

Fig. 7: Test Results for all three proposed algorithms

4 Conclusion

This paper proposed three different lightweight algorithms, in order to accommodate the estimation of a specific area of interest for a semi-autonomous, wildfire recognition quadcopter. The main outcome of the performed tests is that in the case of a real scenario, the first two approaches provide an increased safety distance of the quadcopter from the fire. The *Angled Camera Image Ratio Approach* required that the quadcopter is significantly closer to the area of interest, risking the integrity of the quadcopter. As a result, this approach will provide a slightly lower accuracy than that of the *Front-Facing Image Ratio Approach*, with a difference of $\approx 8\%$. For the purpose of this study, these tests are designed to simulate the input from a DEMA quadcopter collecting thermal imagery, as previously described. Although, before these algorithms can be implemented into real emergency situations, further testing using images and videos from real wildfires is needed in order to test the accuracy on a multitude of situations. Additionally, part of the future directions of this project is to develop a way to determine the wildfires size even if it is not fully included in a single frame and to explore a highly efficient on board algorithm to process the detection and size estimation without the need for a ground computer.

References

1. Amanatiadis, A., Bampis, L., Karakasis, E.G., Gasteratos, A., Sirakoulis, G.: Real-time surveillance detection system for medium-altitude long-endurance unmanned aerial vehicles. Concurrency and Computation: Practice and Experience **30**(7), e4145 (2018), https://doi.org/10.1002/cpe.4145
2. Martínez-de Dios, J., Merino, L., Caballero, F., Ollero, A.: Automatic forest-fire measuring using ground stations and unmanned aerial systems. Sensors **11**(6), 6328–6353 (2011), https://doi.org/10.3390/s110606328
3. Gates, D.: Drone tracks fire hot spots in successful olympic forest test (2015 (accessed 13-02-2019)), https://tinyurl.com/y4egvn9o
4. Hansen, S.M., Pedersen, M.S.: 83 drbt i grske skovbrande (2018 (accessed 04-02-2019)), https://tinyurl.com/y2jnvnvo
5. Lum, C.W., Summers, A., Carpenter, B., Rodriguez, A., Dunbabin, M.: Automatic wildfire detection and simulation using optical information from unmanned aerial systems. Tech. rep., SAE Technical Paper (2015)
6. Mackay, A.: Climate change 2007: impacts, adaptation and vulnerability. contribution of working group ii to the fourth assessment report of the intergovernmental panel on climate change. Journal of Environmental Quality **37**(6), 2407 (2008), https://doi.org/10.2134/jeq2008.0015br
7. Merino, L., Caballero, F., Martinez-de Dios, J., Ollero, A.: Cooperative fire detection using unmanned aerial vehicles. In: Proceedings of the 2005 IEEE international conference on robotics and automation. pp. 1884–1889. IEEE (2005), https://doi.org/10.1109/ROBOT.2005.1570388
8. Park, M.: California fire explodes in size, is now largest in state history (2018 (accessed 04-02-2019)), https://tinyurl.com/y5t7uapf
9. Romps, D.M., Seeley, J.T., Vollaro, D., Molinari, J.: Projected increase in lightning strikes in the united states due to global warming. Science **346**(6211), 851–854 (2014), https://doi.org/10.1126/science.1259100
10. Sandler, M., Howard, A., Zhu, M., Zhmoginov, A., Chen, L.C.: Mobilenetv2: Inverted residuals and linear bottlenecks. In: Proceedings of the IEEE Conference on Computer Vision and Pattern Recognition. pp. 4510–4520 (2018), https://doi.org/10.1109/CVPR.2018.00474
11. Smith, B.: Are drones the future of firefighting? (2014 (accessed 13-02-2019)), https://tinyurl.com/y5yvqv7k
12. Toft, E.: 80 skovbrande i sverige: Nu skal folk forlade et helt omrde (2018 (accessed 04-02-2019)), https://tinyurl.com/dr-sverige
13. Yuan, C., Liu, Z., Zhang, Y.: Vision-based forest fire detection in aerial images for firefighting using uavs. In: 2016 International Conference on Unmanned Aircraft Systems (ICUAS). pp. 1200–1205. IEEE (2016), https://doi.org/10.1109/10.1109/ICUAS.2016.7502546
14. Zhao, Y., Ma, J., Li, X., Zhang, J.: Saliency detection and deep learning-based wildfire identification in uav imagery. Sensors **18**(3), 712 (2018), https://doi.org/10.3390/s18030712